

## Supplementary Materials for

### **The flavonoid cyanidin blocks binding of the cytokine interleukin-17A to the IL-17RA subunit to alleviate inflammation in vivo**

Caini Liu, Liang Zhu, Koichi Fukuda, Suidong Ouyang, Xing Chen, Chenhui Wang, Cun-jin Zhang, Bradley Martin, Chunfang Gu, Luke Qin, Suguna Rachakonda, Mark Aronica, Jun Qin,\* Xiaoxia Li\*

\*Corresponding author. Email: qinj@ccf.org (J.Q.); lix@ccf.org (X.L.)

Published 21 February 2017, *Sci. Signal.* **10**, eaaf8823 (2017)  
DOI: 10.1126/scisignal.aaf8823

#### **This PDF file includes:**

- Fig. S1. A18 binds directly to IL-17RA.
- Fig. S2. A18 specifically inhibits IL-17A–induced gene expression.
- Fig. S3. A18 alleviates T<sub>H</sub>17 cell–mediated, but not T<sub>H</sub>1 cell–mediated, EAE in mice.
- Fig. S4. HFD-induced asthma is attenuated in IL-17RC–deficient mice.
- Fig. S5. HDM- and CFA-induced asthma is alleviated in IL-17RC–deficient mice.
- Fig. S6. Analysis of the C6–C3–C6 flavonoid skeleton and of the hydroxyl groups of A18 that are critical to inhibit IL-17A signaling.

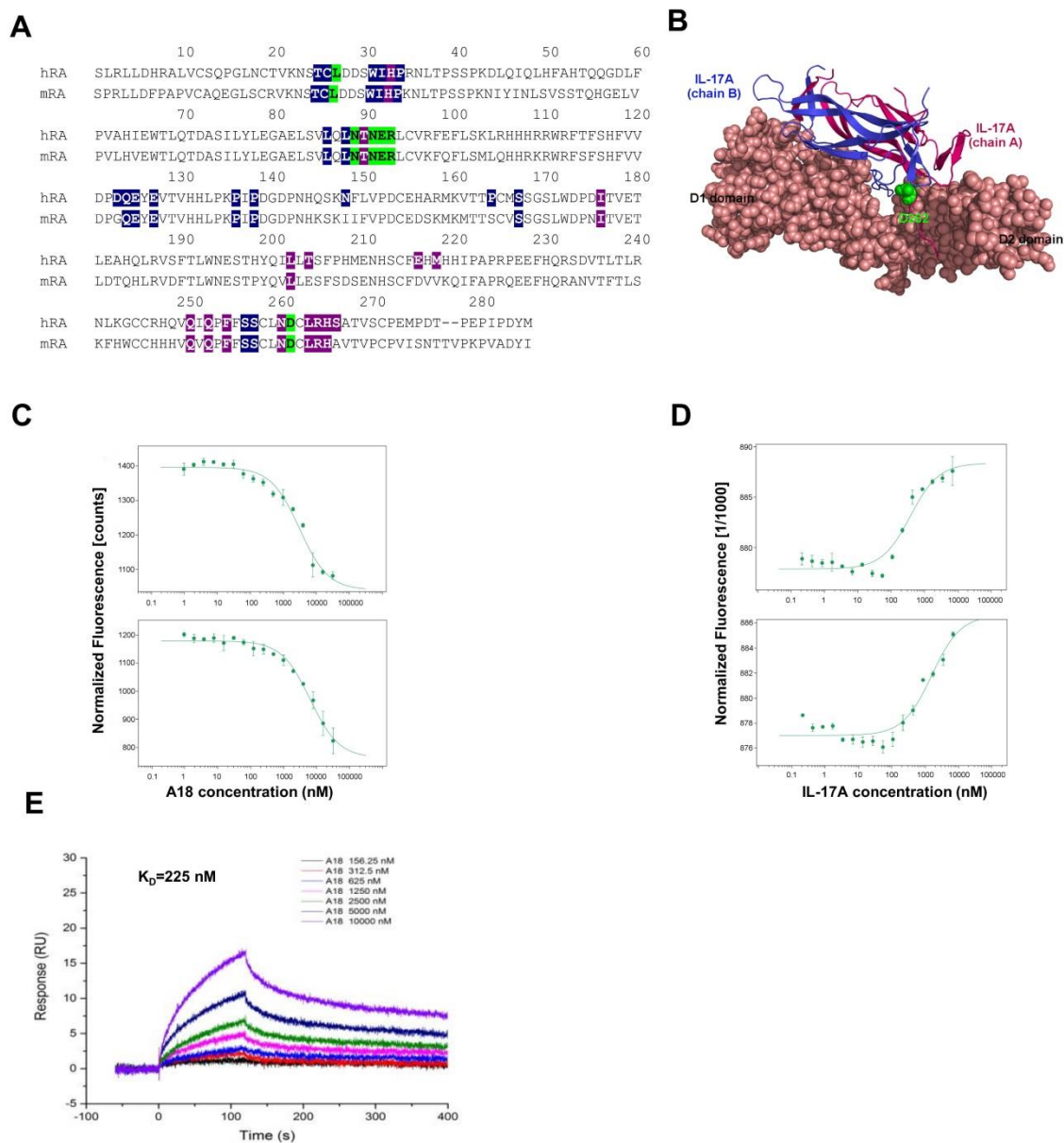


**Fig. S1. A18 binds directly to IL-17RA.** (A) Sequence alignment of the extracellular domains of the human (hRA) and mouse (mRA) IL-17RA proteins. The amino acid residues of human IL-17RA that make contact with IL-17A chain A only, IL-17A chain B only, or both chains are highlighted in violet, dark blue, and green, respectively. Predicted contacts and conserved residues of mouse IL-17 RA are also highlighted accordingly. (B) Crystal structure of the complex formed between human IL-17RA and human IL-17A (PDB: 4HSA). IL-17A is shown as a surface model. The residue Asp<sup>262</sup> (D262) is shown in green. (C) Analysis of the interactions between A18 and either WT IL-17RA (top) or the D262A mutant IL-17RA (bottom) as determined by measurement of the fluorescence changed caused by the binding of A18 to the receptors. (D) Analysis of the interactions between IL-17A and either WT IL-17RA (top) or the D262A IL-17RA mutant (bottom) as determined by microscale thermophoresis (MST). (E) SPR analysis of the binding of A18 to IL-17RA. Solutions of A18 (156.25 to 10,000 nM) were injected over the IL-17RA-immobilized CM5 sensor chip. The binding affinity  $K_D$  was determined by Biaevaluation software. Data in (C) to (E) are means  $\pm$  SEM of three independent experiments.

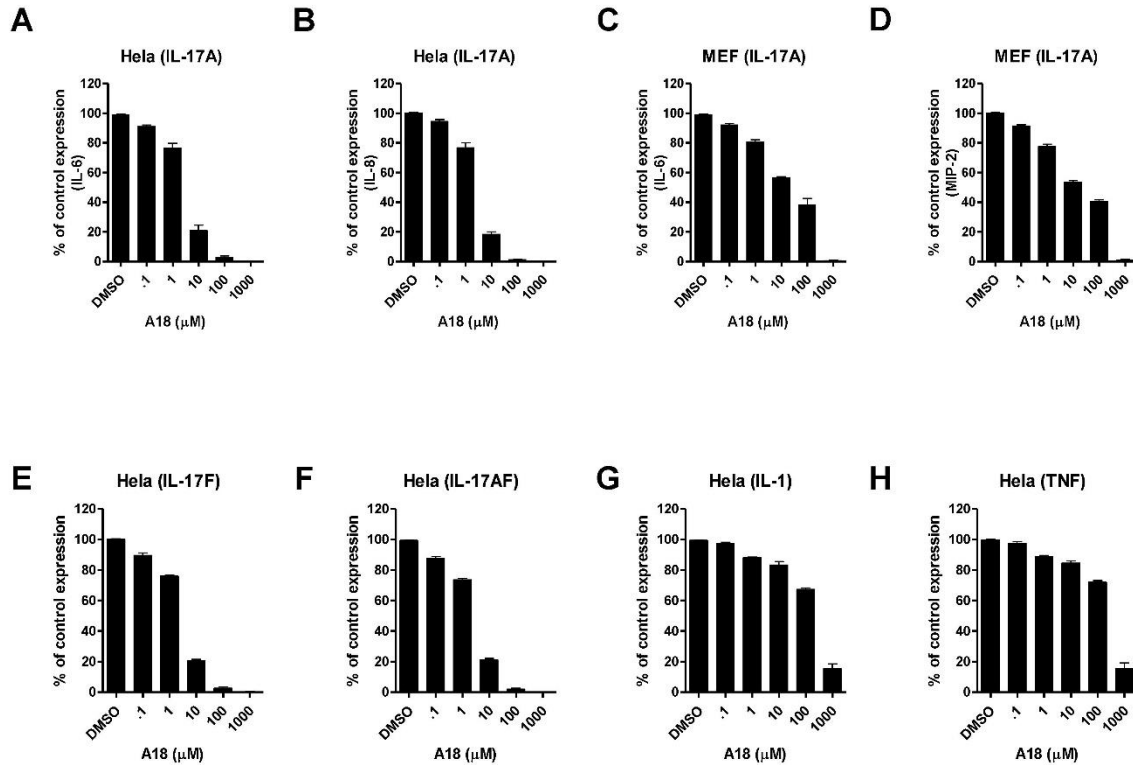


**Fig. S2. A18 specifically inhibits IL-17A–induced gene expression.** (A to D) HeLa cells (A and B) and MEFs (C and D) were treated for 24 hours with IL-17A in the presence of DMSO or the indicated concentrations of A18. The concentrations of the indicated cytokines and chemokines in the culture medium were measured by ELISA. Results are presented as a percentage of the CXCL1 in the medium of IL-17A–stimulated, DMSO-treated cells, which was set at 100%. Data are representative of four independent experiments. The error bars represent the SEM of technical replicates. (E to H) HeLa cells were treated with IL-17F, IL-17A/F (a heterodimer of IL-17A and IL-17F), IL-1, or TNF- $\alpha$  for 24 hours in the presence of DMSO or the indicated concentrations of A18. The concentrations of CXCL1 (GRO $\alpha$  in human and KC in mouse) in the culture medium were measured by ELISA. Results are presented as a percentage of the CXCL1 in the medium of IL-17A–stimulated, DMSO-treated cells, which was set at 100%. Data are representative of four independent experiments. The error bars represent the SEM of technical replicates.

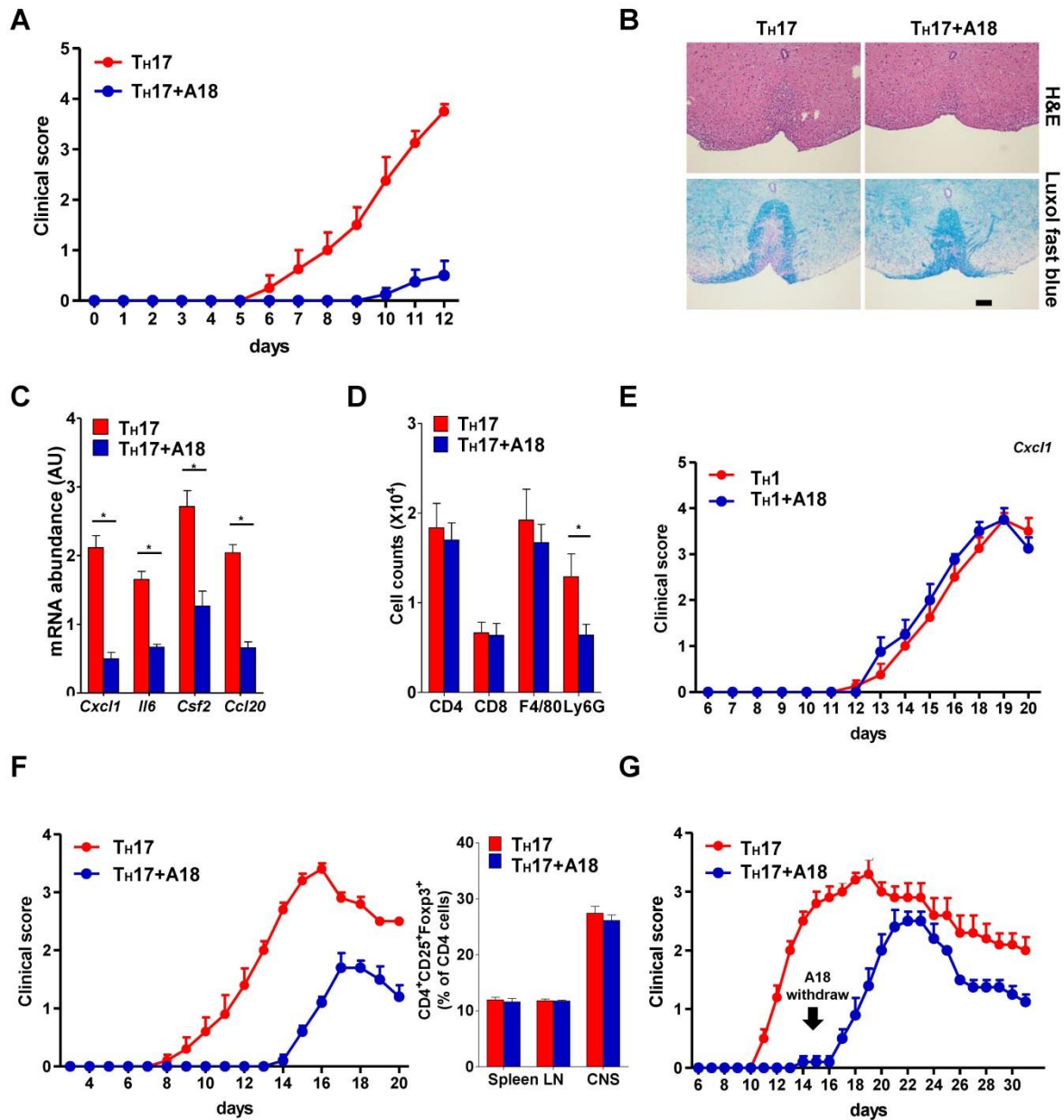


**Fig. S3. A18 alleviates TH17 cell-mediated, but not TH1 cell-mediated, EAE in mice.** (A to G) MOG<sub>33-55</sub>-specific TH17 cells or TH1 cells were adoptively transferred to 10-week-old female C57BL/6J mice that were treated with or without A18. (A) The mean clinical EAE scores of the mice after TH17 cell transfer in the presence or absence of A18 were determined over time. (B) The spinal cords of the indicated mice were subjected to H&E and luxol fast blue staining on day 12 after the adoptive transfer of TH17 cells. Scale bar, 100  $\mu$ m. (C) Spinal cord tissue from the indicated mice was subjected to real-time PCR analysis of the abundances of the indicated mRNAs on day 12 after the adoptive transfer of TH17 cells in the presence or absence of A18. (D) The percentages of CD4<sup>+</sup> T cells, CD8<sup>+</sup> T cells, F4/80<sup>+</sup> macrophages, and Ly6G<sup>+</sup> neutrophils in the brains of the indicated mice were determined by flow cytometric analysis on day 12 after the transfer of the TH17 cells in the presence or absence of A18. (E) The mean clinical EAE

scores of the mice after T<sub>H</sub>1 cell transfer in the presence or absence of A18 were determined over time. (F) Left: The mean clinical EAE scores of the mice after the transfer of T<sub>H</sub>17 cells in the presence or absence of A18 were determined over time. Right: The percentages of CD4<sup>+</sup>CD25<sup>+</sup>Foxp3<sup>+</sup> T<sub>reg</sub> cells in the spleens, lymph nodes (LNs), and CNS of the indicated mice on day 20 after T<sub>H</sub>17 cell transfer were assessed by flow cytometric analysis. (G) Mean clinical EAE scores of the mice after T<sub>H</sub>17 cell transfer in experiments in which A18 was withdrawn at day 15. Data are means ± SEM of eight mice per group from two independent experiments. \**P* < 0.05.

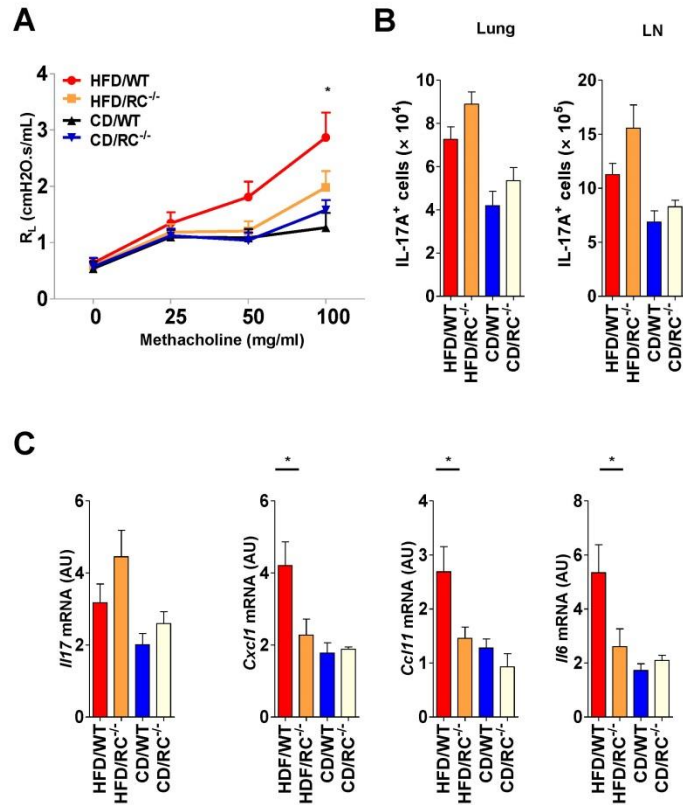


**Fig. S4. HFD-induced asthma is attenuated in IL-17RC-deficient mice.** (A to C) Male C57BL/6J mice (WT) and littermate IL-17RC<sup>-/-</sup> mice were maintained on CD or HFD for 12 weeks starting at 4-weeks of age. (A) At the end of a 12-week diet, lung resistance ( $R_L$ ) in the indicated mice in response to increasing concentrations of aerosolized methacholine was determined. (B) The percentages of IL-17A<sup>+</sup> cells isolated from the lungs and lymph nodes (LN) of the indicated mice were assessed by flow cytometric analysis (C) The lung tissues of the indicated mice were harvested and subjected to real-time PCR analysis of the relative abundances of the indicated mRNAs. Data are means  $\pm$  SEM of five mice per group from each of three independent experiments. \* $P < 0.05$  when comparing WT mice fed a HFD with IL-17RC<sup>-/-</sup> mice fed a HFD.

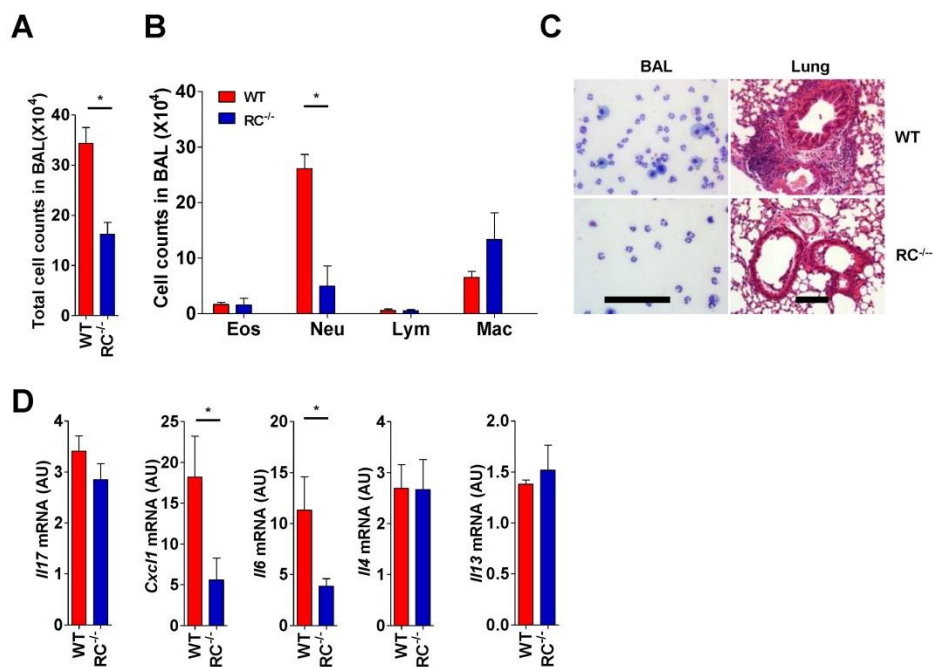


**Fig. S5. HDM- and CFA-induced asthma is alleviated in IL-17RC-deficient mice.** (A to D) Eight-week-old female C57BL/6J mice (WT) and littermate IL-17RC<sup>-/-</sup> mice were sensitized (s.c.) with HDM in CFA on day 0 and subsequently challenged (i.n.) with HDM on day 14. (A and B) Twenty-four hours after challenge, the total numbers of cells (A) and the numbers of the indicated immune cell types (B) in the BAL were counted. (C) BAL cytopins were prepared and lung tissues were subjected to H&E staining. Scale bar, 100 μm. (D) Lung tissues from the indicated mice were subjected to real-time PCR analysis of the relative abundances of the indicated mRNAs. Data are means ± SEM of four mice per group from three independent experiments. \**P* < 0.05 when comparing the HDM-treated mice to the mice treated with HDM and A18.

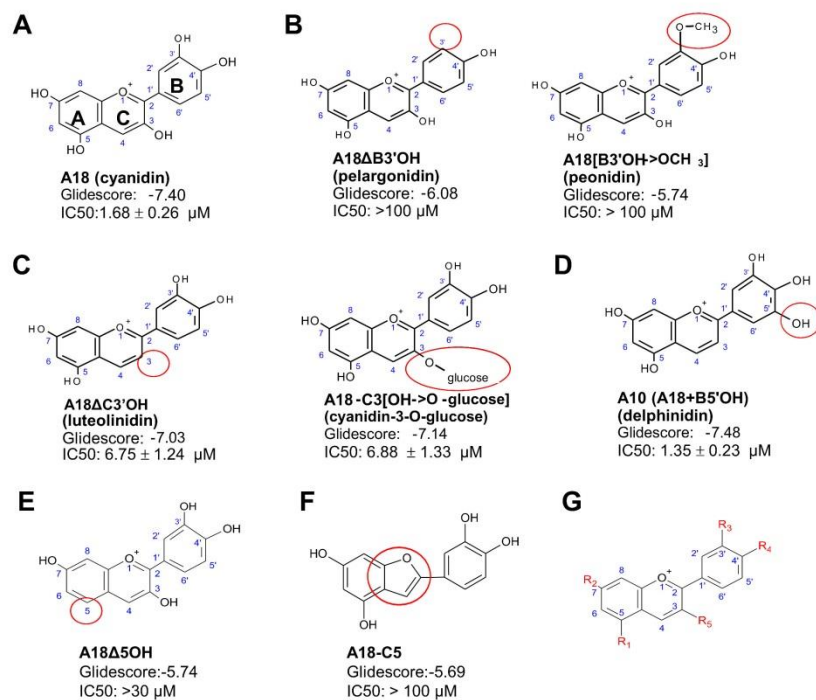


**Fig. S6. Analysis of the C6–C3–C6 flavonoid skeleton and of the hydroxyl groups of A18 that are critical to inhibit IL-17A signaling.** (A to F) Glidescores and IC<sub>50</sub> values of A18 (A) and its structurally related compounds (B to F) were determined as described in Materials and Methods. IC<sub>50</sub> values were calculated from three independent experiments and are expressed as means ± SEM. (G) The basic skeleton that could potentially be used as a prototype for the development of A18-derived, small-molecule drug candidates.